Published in final edited form as:
Inorg Chem. 2009 September 7; 48(17): 8469–8479. doi:10.1021/ic901079s.

Circularly Polarized Luminescence in Enantiopure Europium and Terbium Complexes with Modular, All-Oxygen Donor Ligands

Michael Seitz[†], **King Do**[‡], **Andrew J. Ingram**[‡], **Evan G. Moore**[†], **Gilles Muller**[‡,*], and **Kenneth N. Raymond**[†,*]

[†] Department of Chemistry, University of California, Berkeley, CA 94720-1460, USA

[‡] Department of Chemistry, San José State University, San José, CA 95192-0101, USA

Abstract: Circulaly polarized luminescence from terbium(III) complexed and excited by chiral antenna ligands gives strong emission

The modular synthesis of three new octadentate, enantiopure ligands are reported - one with the bidentate chelating unit 2-hydroxyisophthalamide (IAM) and two with 1-hydroxy-2-pyridinone (1,2-HOPO) units. A new design principle is introduced for the chiral, non-racemic hexamines which constitute the central backbones for the presented class of ligands. The terbium(III) complex of the IAM ligand, as well as the europium(III) complexes of the 1,2-HOPO ligands are synthesized and characterized by various techniques (NMR, UV, CD, luminescence spectroscopy). All species exhibit excellent stability and moderate to high luminescence efficiency (quantum yields Φ_{Eu} = 0.05–0.08 and Φ_{Tb} = 0.30–0.57) in aqueous solution at physiological pH. Special focus is put onto the properties of the complexes in regard to circularly polarized luminescence (CPL). The maximum luminescence dissymmetry factors (g_{lum}) in aqueous solution are high with $|g_{lum}|_{max}$ = 0.08 – 0.40. Together with the very favorable general properties (good stability, high quantum yields, long lifetimes), the presented lanthanide complexes can be considered as good candidates for analytical probes based on CPL in biologically relevant environments.

1 Introduction

The application of luminescence methodology[1] has become widely used in the natural sciences in recent decades. It is particularly important in areas related to biology and medicine, such as genetics, biotechnology, medical diagnostics, and forensics. Lanthanide luminescence occupies a special position within the general field which predominantly features purely organic molecules as luminophores. With the use of lanthanides in aqueous solutions come certain difficulties (e.g. low molar absorptivities, highly labile coordination chemistry, quenching by OH- and NH-oscillators). However once these difficulties are overcome there are also a number of sizeable benefits (long luminescence lifetimes, line-like emission bands, large Stokes shifts). The problems have been overcome to a great extent for several lanthanides (particularly for europium and terbium) in a number of highly efficient systems,[2] some of which have already emerged as commercial products.[3] One of the under-developed unique features of lanthanide luminescence is the feasibility of circularly polarized luminescence (CPL) spectroscopy,[4,5–16] which is the emission analogue of circular dichroism (CD). While in general the observation of CPL is not restricted to chiral lanthanide systems, the effects for chiral organic molecules are usually several orders of magnitude smaller than those for

raymond@socrates.berkeley.edu and gilles.muller@sjsu.edu.

Supporting Information Available. Complete CD and CPL spectra of all lanthanide complexes. This material is available free of charge via the Internet at http://pubs.acs.org.

compounds containing emissive rare-earth elements. For example, a value for the luminescence dissymmetry factor g_{lum} equal to 1×10^{-3} has been measured for chiral triarylamine-based helicenes,[18] whereas lanthanide-containing systems with chiral 2-hydroxyisophthalamide-, pyridyl diamide-, 1-hydroxy-2-pyridinone-, or DOTA-based ligand derivatives exhibited g_{lum} values as high as 0.5.[9–13] Recently, europium complexes with a camphor-based ligand have been reported with extremely high g_{lum} values of up to 1.38.[15] Together with the general advantages of lanthanide luminescence, CPL also offers highly specific information about the chiral environment of the emitting metal complex (e.g. similar solution structures would result in similar CPL patterns including shape, sign and/or magnitude). It should be noted that CPL can also be used to verify if a lanthanide(III) complex solution contains a mixture of diastereomeric species. If only one emitting species contributes to the observed luminescence from the sample, then the CPL results should be independent of the excitation polarization (e.g. right-, left-, or plane-polarized light).[13] Should the solution contain a mixture of diastereomers, the CPL should be dependent on the excitation polarization.[19] This makes CPL a very interesting, specialized extension to the highly sensitive and efficient luminescence methodology.

In this context, we recently introduced the octadentate, enantiopure ligands H_4**1** (Figure 1) for the chelation of terbium(III) and H_4**4** (Figure 2) for europium(III).[11,20] The corresponding complexes showed very promising general luminescence characteristics (high quantum yield, long lifetimes), as well as rather strong CPL activity in aqueous solution at physiological pH. H_4**1** and H_4**4** feature two different organic chromophores/chelators (IAM: 2-hydroxyisophthalamides and 1,2-HOPO: 1-hydroxy-2-pyridinones, respectively) and incorporate the chiral information in two different positions of the hexamine backbone (central trans-1,2-diaminocyclohexane and ethyl substituents in the peripheral ethylene arms, respectively). In order to complete the possible permutations (chromophore and backbone type), we report here the corresponding new ligands H_4**2** (Figure 1) and H_4**3** (Figure 2). In addition, we introduce a modified ligand design with H_4**5** (Figure 2), which is tailor-made for the combination Eu^{3+}/1,2-HOPO. Aside from the synthesis of these new, octadentate chelators and their corresponding lanthanide complexes, this article also reports the luminescence characteristics (general and CPL) for these species.

2 Results and Discussion

2.1 Ligand Design Principle

As reported earlier,[11] the most important structural feature of the new octadentate ligands H_4**X** (**X** = **1**–**5**) is the separation of the chiral information from the chromophore/chelator. This allows for a modular synthesis of an array of chiral ligands, which has considerable advantages (synthetic efficiency, flexibility, etc.) relative to the first-generation IAM-based ligands initially introduced by us (Figure 3).[10] With this new concept it was possible for the first time to obtain an enantiopure, second-generation ligand H_4**4** with the 1,2-HOPO motif, which itself is not easily amenable to the introduction of chiral substituents unlike the IAM moiety with its two amide functionalities.

The complex [Tb(H**1**)] has excellent characteristics: high quantum yield in aqueous solution ($\Phi = 0.57$), no water molecule in the inner coordination sphere of the lanthanide (q = 0), and rather strong CPL activity. The combination of H_4**4** with Eu^{3+} results in a high quantum yield ($\Phi = 0.077$) and shows strong CPL effects, but one water molecule (q = 1) was found to be directly bound to the metal center due to insufficient steric shielding by the ligand from the aqueous bulk solvent.[11] Since our report in this preliminary communication, molecular modeling and a partial crystal structure of a similar complex suggested that a water molecule could access the bottom part of the complex (**III**, Figure 4) due to a lack of appropriate substituents in 3-position on the 1,2-HOPO ring.[21] In the related terbium-IAM complex (**II**,

Figure 3) with q = 0, the methyl amides exert a larger steric influence at the assumed bottom binding site for external H_2O. Further investigation suggested another potential solution to the inner-sphere water coordination in [Eu(H**4**)(H_2O)] (schematic: **III**, Figure 4), which considerably lowers the achievable quantum yields through non-radiative deactivation by vibrational coupling to the nearby O-H oscillators: elongation of two arms of the hexamine backbone from an ethylene-C_2 unit to a propylene-C_3 spacer results in more steric bulk at the lower end of the complex (**IV**, Figure 4). This substantially decreases the exposure of the europium center to bulk water by eliminating the necessary space for H_2O binding.

2.2 Ligand Synthesis

For the realization of this third-generation approach, a new chiral hexamine **10** was prepared as outlined in Scheme 1. Its synthesis started from known, selectively at the primary amines protected bis(trifluoroacetamide) **7**,[22] which already has two propylene-C_3 units attached to the central ethylene moiety. Two-fold regioselective ring-opening of (*R*)-*N*-tosyl-2-ethylaziridine (**8**)[23] by the two secondary amines of **7** gave the unsymmetrically protected hexamine **9**. Simultaneous removal of the tosyl- and trifluoroacetamide-protecting groups by a mixture of conc. HBr and glacial acetic acid, followed by ion-exchange chromatography under strongly basic conditions (Dowex 1×8, HO^- form), yielded the enantiopure hexamine **10** as the monohydrate.

The assembly of the three new ligands H_4**2**, H_4**3**, and H_4**5** was achieved in analogous manner as earlier described for the ligands H_4**1** and H_4**4**. Protected, activated carboxylic acid components of IAM **12**[11] and 1,2-HOPO **14**[24] were coupled with the known backbones **11** and **13**, respectively (Scheme 2).[11] In addition, the new hexamine **10** was combined with 1,2-HOPO derivative **14**. Deprotection under the appropriate conditions (see Scheme 2) yielded the highly polar ligands H_4**2**, H_4**3**, and H_4**5** as the HBr, HCl, or HOAc salts.

2.3 Synthesis of the Lanthanide Complexes

The complexes with the new ligands were prepared following a standard protocol ($LnCl_3$ • 6 H_2O, MeOH, pyridine, reflux) (Scheme 3). Ligand H_4**2** was used in combination with terbium since the IAM motif is known to be an efficient sensitizer for this lanthanide.[10–11,25] 1,2-HOPO ligands, on the other hand, have proven to be suitable antenna moieties for the sensitization of europium.[11,26] Consequently, ligands H_4**3** and H_4**5** were utilized for the synthesis of the complexes with Eu^{3+}.

All complexes are air- and moisture stable, almost colorless solids. [Tb(H**2**)(H_2O)][19,27] shows good solubility in aqueous solution, [Eu(H**3**)(H_2O)] is considerably less soluble in water, and [Eu(H**5**)(H_2O)] dissolves only marginally in H_2O.

2.4 NMR Spectroscopy

Complexation of the enantiopure ligands H_4**X** (**X** = **1**–**5**) to a lanthanide is very likely to introduce new stereogenic elements (e.g. chiral-at-metal or helical twist).[28] This entails the formation of potentially more than one diastereomer (fixed chiral centers in the organic ligand backbone plus variable new stereocenters). Therefore, ^{1}H NMR spectroscopy was used to gain information about the conformers of complex formation. Only [Eu(H**3**)(H_2O)] and [Eu(H**4**)(H_2O)],[11] were suitable for ^{1}H NMR analysis in CD_3OD and gave spectra showing only weak paramagnetic effects.

The other complexes were not soluble enough in aqueous media to obtain meaningful NMR spectra, or because of the very broad paramagnetic spectra were inconclusive.

The aromatic region of both spectra (Figure 5) show only three signals, as would be expected from a 6-substituted 1,2-HOPO motif. The equivalence, however, of all four chelating moieties on the NMR time scale in both cases does not rule out a mixture of rapidly interconverting species, an issue which will be discussed again in the context of the photophysical properties.

2.5 General Photophysical Properties

The absorption spectra for the lanthanide complexes in aqueous 0.1 M Tris buffer at pH 7.4 (except for [Eu(H**5**)(H_2O)] which required the addition of MeOH for solubility reasons) show the characteristic bands in the near-UV region ($\lambda_{max} \approx 337–347$ nm). Upon excitation at or near these maxima, only metal-based emission is observed with the characteristic spectral distribution for the respective lanthanides Tb^{3+} (Figure 6) and Eu^{3+} (Figures 7–8). The photophysical properties of the complexes are summarized in Table 1.

In contrast to the previously reported chelates [Tb(H**1**)] and [Eu(H**4**)(H_2O)] (Table 1, rows 1 and 4),[11] the complexes with the new chromophore-backbone combinations [Tb(H**2**)(H_2O)] and [Eu(H**3**)(H_2O)] (Table 1, rows 2 and 3) do not show single-exponential luminescence decays in H_2O and D_2O. The data could be modeled with two independent lifetimes. In each case, a long-lived major species is present in ca. 80%, as well as a less abundant component (ca. 20%) with considerably shorter lifetime. Determination of the number of H_2O molecules (q) present in the inner coordination sphere of the lanthanides utilizing the observed lifetime differences in deuterated and non-deuterated solvents was done using Parker's empirical equations.[29] Two different hydration states are obtained in both cases. The major component in each case ([Tb(H**2**)(H_2O)]: q = 1.0 and [Eu(H**3**)(H_2O)]: q = 1.2) has one water molecule bound directly to the lanthanide, justifying the simplified abbreviation as [Ln(H**X**)(H_2O)] for the mixture of actually two species. The minor species for the combinations Tb^{3+}/H_4**2** and Eu^{3+}/H_4**3** coincidentally exhibit the same value for q (q = 2.6). The exact nature of the two different emitting species remains unclear. It is significant that the difference in hydration number corresponds to approximately two water molecules, which in turn would mean that one bidentate chelating moiety (IAM or 1,2-HOPO) is replaced by the solvent under retention of the coordination number.

The suboptimal shielding of the lanthanide centers from bulk solvent molecules also results in a drop of the quantum yields for these complexes relative to their respective analogues with the same chromophore units ($\Phi = 0.30$ for [Tb(H**2**)(H_2O)] vs. $\Phi = 0.57$ for [Tb(H**1**)] and ($\Phi = 0.048$ for [Eu(H**3**)(H_2O)] vs. $\Phi = 0.077$ for [Eu(H**4**)(H_2O)]). Unfortunately, [Eu(H**5**)(H_2O)] with the newly introduced unsymmetric ligand design cannot directly be compared with the other two europium complexes due to its insufficient solubility in 0.1 M Tris buffer at pH 7.4. Admixture of MeOH (9:1, MeOH/buffer, v/v), however, permitted the measurement of the photophysical properties of this complex in an environment with an aqueous component. The monoexponential lifetime in this medium ($\tau = 0.57$ ms, Table 1, last row) is slightly higher than the one for the successful second-generation europium complex [Eu(H**4**)(H_2O)] in pure Tris buffer ($\tau = 0.48$ ms, Table 1, row 5). The quantum yield for [Eu(H**5**)(H_2O)] is respectable ($\Phi = 0.081$) and essentially the same compared to [Eu(H**4**)(H_2O)] ($\Phi = 0.077$). For both complexes, it is highly likely that water is the most competitive ligand for coordination to the lanthanide. The increase in luminescence lifetime for [Eu(H**5**)(H_2O)] can be explained either by reduced average accessibility of H_2O molecules to the central metal or by a decreased outer-sphere quenching ability of bulk MeOH compared to water. Since it was not possible to perform q-measurements in an aqueous system for [Eu(H**5**)(H_2O)], these were studied in pure MeOH and CD_3OD (Table 1, last row). In these media, the original empirical equation by Horrocks[30] gives a value of q = 0.57. As discussed elsewhere,[29] this treatment does not take into account the potentially considerable quenching effects of nearby X-H (X = O, N, C) oscillators which are not directly bound to the europium cation. Since, there are four amide

hydrogens in close proximity to the metal center, the value is very likely an overestimate and it is likely that methanol molecules do not access the inner coordination sphere. However, while the third-generation ligand design outlined in section 2.1 is very promising, in an aqueous environment with the much smaller ligand H_2O, it seems probable based on the similarities in quantum yield and lifetimes when compared to [Eu(H**4**)(H_2O)] that one water molecule is still bound to the lanthanide in [Eu(H5)(H_2O)].

In summary, from a general luminescence perspective there seems to be a best combination for each of the two lanthanides in terms of backbone-chelator permutations in H_4**X** (with **X** = **1**–**4**). For terbium/IAM the cyclohexane-based scaffold in H_4**1** is clearly superior to the one with the hexamine backbone with four ethyl-substituents in the peripheral arms (in H_4**2**). The combination europium/1,2-HOPO, on the other hand, shows exactly the converse relationship between backbone nature and luminescence behavior, with H_4**4** as the better choice. The new third-generation ligand H_4**5**, though suffering from slight solubility problems of the europium complex, seems to be a promising alternative to the already successful H_4**4**.

2.6 Chiroptical Properties

CD spectroscopy could be performed on MeOH solutions of all complexes. All compounds show Cotton effects in the range 300–390 nm (See Supporting Information).

CPL spectra were obtained for the complexes with H_4**X** (with **X** = **1**–**2**, **4**) in 0.1 M Tris buffer at pH 7.4, whereas [Eu(H**3**)(H_2O)] and [Eu(H**5**)(H_2O)] had to be measured in MeOH. For the terbium complexes the $^5D_4 \rightarrow {}^7F_5$ transitions (at $\lambda \approx 545$ nm) were chosen, for the europium compounds the corresponding emission transition $^5D_0 \rightarrow {}^7F_1$ (at $\lambda \approx 593$ nm). These transitions are magnetic-dipole-allowed (selection rule: $\Delta J = 0, \pm 1$; except $J = 0 \rightarrow J = 0$), which have been shown to be the most likely to yield large circular polarization.[31] The magnitude of the CPL effect is commonly expressed by the luminescence dissymmetry factor g_{lum} which is defined as:

$$g_{lum} = \frac{\Delta I}{\frac{1}{2} I} = \frac{I_L - I_R}{\frac{1}{2}(I_L + I_R)}$$

Here I_L and I_R refer to the intensity of left and right circularly polarized emissions, respectively. Table 2 summarize the CPL data for all five complexes [Ln(H**X**)(H_2O)$_y$] (**X** = **1**–**5**, y = 0, 1). Figure 9 shows as a typical example the CPL spectra for [Tb(H**2**)(H_2O)] (complete CPL spectra of all complexes can be found in the Supporting Information).

All complexes show CPL activities for the transitions investigated ($^5D_4 \rightarrow {}^7F_5$ for Tb^{3+} and $^5D_0 \rightarrow {}^7F_1$ for Eu^{3+}) in MeOH and, where possible, also in aqueous 0.1 M Tris buffer, pH 7.4.

The CPL spectra of [Tb(H**1**)] in aqueous buffer and in MeOH are almost identical, suggesting very similar chiral structures (e.g. comparable chiral arrangement of ligands surrounding the luminescent metal center) in the two different media (Figure S3). The g_{lum} values (Table 2) in aqueous solution are a little higher than the ones in MeOH ($|g_{lum}| = 0.033 – 0.083$). The CPL spectra in MeOH are comparable when either a direct excitation of Tb^{3+} ($\lambda_{exc} = 488$ nm) or an indirect excitation through the ligand absorption bands ($\lambda_{exc} = 352$ nm) is used. In order to establish the number of emitting species in solution, we also performed experiments in MeOH with a direct circularly polarized excitation (CPE) of the Tb^{3+} center. In every case (left-, right-, and plane-polarized) the CPL activities were identical, strongly indicating only one, and hence diastereopure luminescent species. This finding is in good agreement with the observation of a monoexponential luminescence decay for [Tb(H**1**)] in aqueous buffer (see Table 1).

For [Tb(H**2**)(H_2O], in contrast to [Tb(H**1**)], the shape and amplitude of the CPL activities in aqueous buffer and in MeOH are different (Figure 9). Surprisingly, the absolute values for g_{lum} in Tris buffer are very high and almost an order of magnitude greater than the ones in MeOH ($|g_{lum}|_{max}$ = 0.40 vs. $|g_{lum}|_{max}$ = 0.041). Although the reason for this increase remains unclear, we suggest that the chiral structure of [Tb(H**2**)(H_2O)] is solvent-dependent. As has been seen for the lifetime measurements in section 2.5 (Table 1: biexponential decay), more than one emitting species can be expected in solution. This result is also supported by the following two findings in MeOH: a) Different g_{lum} values are obtained upon direct excitation of Tb^{3+} (λ_{exc} = 488 nm) or after indirect excitation through the ligand (λ_{exc} = 360 nm); b) The g_{lum} values were dependent on the polarization of the excitation beam (left-, right-, and plane-polarized) upon direct excitation of Tb^{3+}, a clear sign for the presence of multiple emitting species due to the presence of a mixture of diastereomeric species and/or species with partial decomplexation of the ligand arms.

Of the three Eu(III) complexes, only [Eu(H**4**)(H_2O] was soluble enough in aqueous Tris buffer for CPL measurements. For this compound, the CPL spectra in aqueous solution and in MeOH are very similar (Figure S6) with high maximum g_{lum} values (Table 2: 0.1 M Tris, pH 7.4: −0.12 vs. MeOH: −0.20). The absolute maximum magnitude of the dissymmetry factor is comparable in methanolic solutions of [Eu(H**3**)(H_2O] (Table 2: g_{lum} = −0.17) and [Eu(H**5**)(H_2O] (Table 2: g_{lum} = −0.12). The similarity between the CPL spectra of [Eu(H**3**)(H_2O] and [Eu(H**5**)(H_2O] (Figures S5 and S7) suggests that both complexes adopt a relatively comparable structure, whereas the Eu(III) chiral environment in [Eu(H**4**)(H_2O] (Figure S6) is different from the former complexes. These results indicate that the sign and magnitude of the CPL is primarily controlled by the chiral arrangement of ligands surrounding the luminescent metal center and, therefore, by the nature of the chiral substituents. Unfortunately, all three complexes could not be investigated by means of CPL following circularly polarized excitation (CPE) due to continued precipitation of the compounds when placed in the laser excitation beam.

3 Conclusions

In summary, a new family of enantiomerically pure, octadentate ligands provides excellent stability and favorable photophysical properties for trivalent lanthanide cations in aqueous solution. In particular:

1. The modular nature of the ligand syntheses allows for facile and efficient assembly of the chiral oligoamine backbone with achiral chelators/antenna chromophores. The capability of varying these two building blocks independently makes it possible to generate molecular diversity very rapidly and will thus enables combinatorial screening for successful ligand lead structures for CPL applications in the future.
2. The europium(III) and terbium(III) complexes of the corresponding ligands show good to excellent general luminescence properties in aqueous solution. For each of the two lanthanides, there is an optimal combination of the modular ligand building blocks which ensures the existence of only one emitting species and high quantum yields Φ of up to 0.57 for terbium and 0.08 for europium.
3. The magnitudes of the CPL effects are high for all compounds ($|g_{lum}|$ of up to 0.40 for terbium and $|g_{lum}|$ of up to 0.20 for europium) and are potentially promising for the use of these new complexes in analytical/sensing applications in the future. The combination of lifetime and CPL/CPE measurements strongly suggested the presence of single or multiple species in solution. Of special importance is that these two spectroscopic techniques were able to provide the necessary pieces of information when NMR was not conclusive.

4 Experimental Section

4.1 General

Chemicals were purchased from commercial suppliers and used as received unless stated otherwise. Solvents were dried by standard procedures (benzene: Na-wire, MeOH: Mg/I_2). Pyridine was distilled before use. Elemental analyses and mass spectrometry were performed by the microanalytical and mass spectrometry facilities of the University of California, Berkeley. NMR spectra were measured on Bruker AVQ-400 (^{1}H: 400 MHz, ^{13}C: 101 MHz) and DRX-500 (^{1}H: 500 MHz).

4.2 Ligand Synthesis

Protected ligand $H_4$2 • 3 H_2O—(*R*,*R*,*R*,*R*)-N,N,N′,N′-tetrakis(2-aminobutyl)-1,2-diaminoethane hydrate (**11**) (430 mg, 1.19 mmol, 1.0 equiv.) was dissolved in dry CH_2Cl_2 (15 mL). NEt_3 (631 mg, 6.24 mmol, 5.0 equivs.) and the monothiazolide **12** (2.14 g, 6.89 mmol, 5.5 equivs.) were added subsequently and the solution was heated to reflux for 17 h. The solvent was removed and the yellow residue was subjected to column chromatography (SiO_2, CH_2Cl_2/MeOH 50:1 to CH_2Cl_2/MeOH 9:1). The fractions with R_f = 0.36 (TLC, SiO_2, CH_2Cl_2/MeOH 9:1, UV detection) were concentrated to yield a colorless solid (540 mg, 39%).

Mp. 87–92°C. ^{1}H-NMR (400 MHz, $CDCl_3$): δ = 7.73 (dd, *J* = 7.7, 1.9 Hz, 4 H), 7.58-7.47 (m, 8 H), 7.24 (dd, *J* = 7.7, 1.9 Hz, 4 H), 6.86 (t, *J* = 7.7 Hz, 4 H), 4.25-4.05 (m, 4 H), 3.68 (s, 12 H), 2.93 (d, *J* = 4.9 Hz, 12 H), 2.65-2.46 (m, 12 H), 1.80-1.63 (m, 4 H), 1.60-1.44 (m, 4 H), 1.01 (t, *J* = 7.5 Hz, 12 H) ppm. ^{13}C-NMR (100.6 MHz, $CDCl_3$): δ = 166.0, 165.7, 155.5, 133.3, 132.7, 128.3, 128.0, 124.3, 63.0, 58.9, 51.0, 48.8, 26.7, 26.5, 10.5 ppm. MS (FAB+): m/z (%) = 1109.8 (100, $[M+H]^+$), 859.5 (70), 554.3 (66). Anal. Calcd. (Found) for $C_{58}H_{80}N_{10}O_{12}$ • 3 H_2O (M_r = 1163.36): C, 59.88 (59.90); H, 7.45 (7.27); N, 12.04 (12.18).

$H_4$2 • 4 HBr • 2 H_2O—Under argon, the protected ligand H_4**2** • 3 H_2O (460 mg, 395 μmol, 1.0 equiv.) was dissolved in dry CH_2Cl_2 (20 mL) and the solution was cooled down to −50°C (external temperature). BBr_3 (2.0 mL, 5.3 g, 21.2 mmol, 54 equivs.) was added dropwise and the cooling-bath was removed. The yellow suspension was stirred at ambient temperature for 84 h. The yellow suspension was concentrated under vacuum and cooled in an ice-bath. MeOH (50 mL) was added cautiously, the ice-bath was removed, and the yellow solution was refluxed for 10 h. The solvents was evaporated and the light-brown solid dried under reduced pressure at 40°C (bath temperature) for 16 h. The deprotected ligand was obtained as a light-brown powder (350 mg, 63%) that was used without further purification.

^{1}H-NMR (400 MHz, CD_3OD): δ = 7.87-7.52 (m, 8 H), 6.72-6.57 (m, 4 H), 4.66-4.53 (m, 2 H), 4.47-4.32 (m, 2 H), 4.25-4.13 (m, 2 H), 4.09-3.98 (m, 2 H), 3.91-3.78 (m, 4 H), 3.72-3.52 (m, 4 H), 2.93-2.83 (m, 14 H), 1.95-1.62 (m, 10 H), 1.19-0.92 (m, 16 H) ppm. ^{13}C-NMR (100.6 MHz, CD_3OD): δ = ppm. MS (FAB+): m/z (%) = 1053.7 (100, $[M+H]^+$), 526.2 (21). Anal. Calcd. (Found) for $C_{54}H_{72}N_{10}O_{12}$ • 4 HBr • 2 H_2O (M_r = 1412.89): C, 45.90 (45.86); H, 5.71 (5.72); N, 9.91 (9.78)..

Protected ligand $H_4$3 • 2.5 H_2O—(*R*,*R*)-N,N,N′,N′-tetrakis(2-aminoethyl)-1,2-diaminocyclohexane hydrate (**13**) (520 mg, 1.71 mmol, 1.0 equiv.) and NEt_3 (1.38 g, 13.6 mmol, 8.0 equivs.) were dissolved in dry CH_2Cl_2 (40 mL), cooled to 0°C, and a solution of the acid chloride **14** (2.47 g, 9.37 mmol, 5.5 equivs.) was added in CH_2Cl_2 (40 mL). The solution was stirred at ambient temperature for 40 h. The organic phase was washed with sat. Na_2CO_3 (80 mL) and brine (80 mL), dried ($MgSO_4$), and concentrated. The dark brown residue was purified by column chromatography (SiO_2, CH_2Cl_2/MeOH 100:1 to CH_2Cl_2/MeOH 10:1).

The fraction with R_f = 0.43 (TLC, SiO_2, CH_2Cl_2/MeOH 10:1) was collected and concentrated to yield a light-brown solid (1.23 g, 58%).

Mp. 114–118 °C. ^{1}H-NMR (400 MHz, $CDCl_3$): δ = 7.65-7.39 (m, 12 H), 7.36-7.17 (m, 16 H), 6.72-6.58 (m, 4 H), 6.30-6.17 (m, 4H), 5.35-5.19 (m, 8 H), 3.52-2.80 (m, 8 H), 2.74-2.22 (m, 8 H), 2.19-2.00 (m, 2 H), 1.91-1.50 (m, 4 H), 1.21-0.67 ppm. ^{13}C-NMR (100.6 MHz, $CDCl_3$): δ = 160.6, 158.4, 142.7, 138.3, 133.3, 130.2, 129.4, 128.6, 123.9, 105.6, 79.3, 61.2, 39.0, 25.5, 24.8 ppm. MS (FAB+): m/z (%) = 1195.8 (100, $[M+H]^+$), 1087.8 (70, [M-OBn +H]$^+$). Anal. Calcd. (Found) for $C_{66}H_{70}N_{10}O_{12}$ • 2.5 H_2O (M_r = 1240.36): C, 63.91 (63.92); H, 6.09 (5.91); N, 11.29 (11.50).

$H_4$3 • 2 HCl • 3 HOAc • 4 H_2O—The protected ligand H_4**3** • 2.5 H_2O (0.76 g, 613 μmol, 1.0 equiv.) was dissolved in a mixture of conc. HCl (30 mL) and glacial HOAc (30 mL). The solution was stirred at ambient temperature for 84 h and at 50°C for additional 15 h. The mixture was filtered and the volatiles were removed under reduced pressure at 50 °C. The product was obtained as a pale yellow solid (0.53 g, 74%).

Mp. 84–88 °C. ^{1}H-NMR (400 MHz, DMSO-d_6): δ = 9.29 (br, 4 H), 7.42-7.31 (m, 8 H), 6.57 (dd, *J* = 8.9, 1.5 Hz, 4 H), 6.43-6.26 (br, 4 H), 3.91-3.39 (m, 8 H), 3.32-3.05 (m, 8 H), 2.92-2.67 (m, 2 H), 2.12-1.92 (m, 2 H), 1.82-1.58 (m, 2 H), 1.52-1.11 (m, 4 H) ppm. ^{13}C-NMR (100.6 MHz, DMSO-d_6): δ = 161.2, 157.9, 142.0, 137.6, 120.2, 104.8, 80.8, 61.6, 37.1, 24.7, 24.2 ppm. MS (FAB+): m/z (%) = 835 (100, $[M+H]^+$). Anal. Calcd. (Found) for $C_{38}H_{46}N_{10}O_{12}$ • 2 HCl • 3 HOAc • 4 H_2O (M_r = 1177.99): C, 44.86 (44.73); H, 5.99 (5.60); N, 11.89 (12.04).

(*R*,*R*)-*N*,*N*′-bis[2-(tosylamino)butyl]-*N*,*N*′-bis[3-(trifluoroacetamido)propyl]-1,2-diaminoethane (8)—*N*,*N*′-Bis[3-(trifluoroacetamido)propyl]-1,2-diaminoethane[22] (**7**) (9.71 g, 26.5 mmol, 1.0 equiv.) and (*R*)-*N*-tosyl-2-ethylaziridine[23] (**8**) (13.74 g, 61.0 mmol, 2.3 equivs.) were dissolved in dry benzene (150 mL) and the solution was heated under reflux for 43 h. After cooling down to ambient temperature, the solvent was removed under reduced pressure and the yellow oil was purified by column chromatography (SiO_2, gradient: CH_2Cl_2/MeOH 100:1 to CH_2Cl_2/MeOH 50:1). The fractions with R_f = 0.32 (TLC: SiO_2, CH_2Cl_2/MeOH 20:1, UV detection) were collected, concentrated, and the colorless, very thick oil dried in vacuo at 70°C (bath temperature) for 10 h. The product was obtained as a glass-like colorless solid (12.08 g, 56%).

Mp. 45–48°C. ^{1}H-NMR (400 MHz, $CDCl_3$): δ = 7.87-7.64 (m, 6 H), 7.39-7.23 (m, 4 H), 5.53 (br s, 2 H), 3.43-3.14 (m, 6 H), 2.80-2.22 (m, 18 H), 1.97-1.58 (br s, 4 H), 1.48-1.33 (m, 4 H), 0.74-0.62 (m, 6 H) ppm. ^{13}C-NMR (100.6 MHz, $CDCl_3$): δ = 157.5 (q, *J* = 38 Hz), 143.5, 137.9, 129.7, 126.9, 115.9 (q, *J* = 287 Hz), 57.8, 53.4, 53.0, 51.9, 51.6, 38.3, 25.8, 25.6, 21.5, 9.1 ppm. MS (FAB+): m/z (%) = 817 (100, $[M+H]^+$), 661 (34), 422 (27), 408 (39). Anal. Calcd. (Found) for $C_{34}H_{50}F_6N_6O_6S_2$ (M_r = 816.92): C, 49.99 (49.93); H, 6.17 (6.16); N, 10.29 (10.11). .

(*R*,*R*)-*N*,*N*′-Bis(2-aminobutyl)-*N*,*N*′-bis(3-aminopropyl)-1,2-diaminoethane hydrate (10)—Under argon, (*R*,*R*)-*N*,*N*′-bis[2-(tosylamino)butyl]-*N*,*N*′-bis[3-(trifluoroacetamido)propyl]-1,2-diamino-ethane (**9**) (12.04 g, 14.7 mmol, 1.0 equiv.) was dissolved in glacial HOAc (80 mL) and aq. HBr (48%, 90 mL) and phenol (1.39 g, 14.77 mmol, 1.0 equiv.) was added. The mixture was heated under reflux for 48 h, cooled down, and allowed to stand at ambient temperature overnight. The supernatant solution was decanted from the dark precipitate and concentrated under reduced pressure. The dark residue was dissolved in water (ca. 50 mL) and purified by ion-exchange chromatography (Dowex 1×8–50, OH^- form). The column was eluted with Millipore water and fractions that tested basic against litmus paper

were combined and evaporated under reduced pressure (bath temperature < 50°C). The product was obtained as a light-yellow oil (2.65 g, 54%).

^{1}H-NMR (400 MHz, D_2O): δ = 2.82-2.69 (m, 2 H), 2.67-2.33 (m, 14 H), 2.31-2.20 (m, 2 H), 1.66-1.31 (m, 6 H), 1.28-1.11 (m, 2 H), 0.86 (t, *J* = 7.3 Hz, 6 H) ppm. ^{13}C-NMR (100.6 MHz, D_2O): δ = 60.6, 52.4, 50.9, 49.6, 39.0, 28.3, 27.4, 9.6 ppm. MS (FAB+): m/z (%) = 317 (100, $[M+H]^+$). Anal. Calcd. (Found) for $C_{16}H_{40}N_6 \cdot H_2O$ (M_r = 334.54): C, 57.44 (57.46); H, 12.65 (13.12); N, 25.12 (24.87). .

The enantiopurity of this material was confirmed as described earlier by ^{1}H-NMR spectroscopy after transformation to the corresponding tetrakis(urea) derivative using (*R*)-1-phenyl-ethylisocyanate.[11]

Protected ligand $H_4$5 • H_2O—(*R*,*R*)-*N*,*N*′-Bis(2-aminobutyl)-*N*,*N*′-bis(3-aminopropyl)-1,2-diaminoethane hydrate (**10**) (320 mg, 837 μmol, 1.0 equiv.) and NEt_3 (0.70 mL, 508 mg, 5.02 mmol, 6.0 equivs.) were dissolved in dry CH_2Cl_2 (20 mL), cooled to 0°C, and a solution of the acid chloride **14** (0.99 g, 3.77 mmol, 4.5 equivs.) was added in CH_2Cl_2 (10 mL). The solution was stirred at ambient temperature for 15 h. An aqueous saturated solution Na_2CO_3 (50 mL) was added cautiously, the phases were separated, and the aqueous phase was extracted with 2 × 20 mL CH_2Cl_2. The combined organic phases were dried ($MgSO_4$) and concentrated. The residue was subjected to column chromatography (SiO_2, gradient: CH_2Cl_2/MeOH 20:1 to CH_2Cl_2/MeOH 9:1). The fractions with R_f = 0.32 (TLC, SiO_2, CH_2Cl_2/MeOH 9:1, UV detection) were collected and concentrated. The product was obtained as colorless solid (350 mg, 34%). Mp. 94–96 °C. ^{1}H-NMR (400 MHz, $CDCl_3$): δ = 7.64-7.14 (m, 26 H), 7.01 (d, *J* = 8.6 Hz, 2 H), 6.66-6.55 (m, 4 H), 6.27 (dd, *J* = 6.7, 1.6 Hz, 2 H), 6.16 (dd, *J* = 6.7, 1.4 Hz, 2 H), 5.40-5.15 (m, 8 H), 3.94-3.74 (m, 2 H), 3.28-2.98 (m, 4 H), 2.42-1.99 (m, 12 H), 1.55-1.13 (m, 8 H), 0.80 (t, *J* = 7.3 Hz, 6 H) ppm. ^{13}C-NMR (100.6 MHz, $CDCl_3$): δ = 160.50, 160.46, 158.5, 147.7, 143.0, 142.9, 138.17, 138.15, 133.4, 133.3, 130.5, 130.2, 129.35, 129.33, 128.50, 128.46, 123.8, 123.7, 105.3, 79.3, 77.2, 58.2, 51.9, 51.4, 50.3, 38.1, 26.1, 25.9, 10.4 ppm. MS (FAB+): m/z (%) = 1225.5 (100, $[M+H]^+$), 1119.7 (29, $[M-OBn+H]^+$), 939.5 (71), 612.3 (48). Anal. Calcd. (Found) for $C_{68}H_{76}N_{10}O_{12} \cdot H_2O$ (M_r = 1243.41): C, 65.68 (65.47); H, 6.32 (6.39); N, 11.26 (11.25). .

$H_4$5 • 2 HCl • 2 HOAc • 6 H_2O—The benzyl protected ligand (230 mg, 185 μmol, 1.0 equiv.) was dissolved in a mixture of conc. HCl (8 mL) and glacial HOAc (8 mL). The solution was stirred at ambient temperature for 72 h. The volatiles were removed under reduced pressure at 35 °C. The product was obtained as a light-brown solid (210 mg, 97%).

Mp. 104–110°C (decomp.). ^{1}H-NMR (400 MHz, DMSO-d_6): δ = 9.12-8.85 (m, 4 H), 7.41-7.30 (m, 4 H), 6.69-6.59 (br, 2 H), 6.58-6.49 (m, 4 H), 6.35 (d, *J* = 5.5 Hz, 2 H), 4.34-4.13 (m, 2H), 3.89-3.57 (m, 4 H), 3.45-3.06 (m, 12 H), 2.12-1.91 (m, 4 H), 1.74-1.58 (m, 2 H), 1.56-1.39 (m, 2 H), 0.89 (t, *J* = 7.3 Hz, 6 H) ppm. ^{13}C-NMR (100.6 MHz, DMSO-d_6): δ = 172.4, 161.2, 160.9, 157.9, 142.5, 142.2, 137.8, 137.7, 120.2, 120.0, 104.9, 104.3, 55.9, 51.5, 47.0, 36.7, 26.3, 22.9, 21.5, 10.4 ppm. MS (FAB+): m/z (%) = 865 (100). Anal. Calcd. (Found) for $C_{40}H_{52}N_{10}O_{12}$ • 2 HCl • 2 HOAc • 6 H_2O (M_r = 1166.02): C, 45.32 (44.99); H, 6.40 (5.98); N, 12.01 (12.07).

4.2 Complex Synthesis

[Tb(H2)(H_2O)] • 2 MeOH • 5 H_2O—The ligand H_4**2** • 4 HBr • 2 H_2O (117 mg, 82.8 μmol, 1.0 equiv.) was dissolved in dry MeOH (5 mL), $TbCl_3$ • 6 H_2O (42 mg, 112 μmol, 1.35 equivs.) and pyridine (512 mg) were added and the mixture was heated under reflux for 14.5 h. The solution was cooled to ambient temperature, water (8 mL) was added dropwise with stirring and the mixture was allowed to stand for 3 h. The formed precipitate was collected on a

membrane filter (Nylon 66, 0.45 μm pore size), washed with ice-cold water, and dried in vacuo at 45°C (bath temperature) for 16 h. The terbium complex was obtained as a pale-yellow solid (43 mg, 38%).

Anal. Calcd. (Found) for $C_{54}H_{69}N_{10}O_{12}Tb \cdot 2\ MeOH \cdot 6\ H_2O$ (M_r = 1381.29): C, 48.69 (48.79); H, 6.49 (6.60); N, 10.14 (9.81).

[Eu(H3)(H_2O)] • MeOH • 2 H_2O—The ligand H**3** • 2 HCl • 3 HOAc • 4 H_2O (290 mg, 246 μmol, 1.0 equiv.) was suspended in a mixture of dry MeOH (10 mL). $EuCl_3 \cdot 6\ H_2O$ (90.2 mg, 246 μmol, 1.0 equiv.) and pyridine (460 mg) were added and the cloudy mixture was refluxed for 21 h. The suspension was cooled down to ambient temperature, the fine solid was collected on a membrane filter (Supelco Nylon 66, 0.45 μm pore size), washed with ice-cold MeOH, and dried under reduced pressure at 50°C (bath temperature) for 18 h. The product was obtained as a light-brown solid (256 mg, 98%).

Mp. >200°C. Anal. Calcd. (Found) for $C_{38}H_{43}EuN_{10}O_{12} \cdot 3\ H_2O \cdot MeOH$ (M_r = 1069.86): C, 43.78 (43.40); H, 4.99 (4.72); N, 13.09 (12.77). .

[Eu(H5)(H_2O)] • 5 H_2O—The ligand H**5** • 2 HCl • 2 HOAc • 6 H_2O (54 mg, 46 μmol, 1.0 equiv.) was dissolved in MeOH (10 mL). Solid $EuCl_3 \cdot 6\ H_2O$ (18 mg, 49 μmol, 1.0 equiv.) and pyridine (115 mg) were added and the mixture was refluxed for 19 h. The suspension was cooled to ambient temperature and the solid was collected, washed with MeOH, and dried in vacuo to give a colorless solid (50 mg, 96%).

Mp. >200°C. Anal. Calcd. (Found) for $C_{40}H_{49}EuN_{10}O_{12} \cdot 6\ H_2O$ (M_r = 1121.93): C, 42.82 (42.92); H, 5.48 (5.20); N, 12.48 (12.3).

4.3 Spectroscopy

UV-Visible absorption spectra were recorded on a Varian Cary 300 double beam absorption spectrometer using quartz cells (1 cm) path. CD spectra were measured on a JASCO J-810 spectropolarimeter using quartz cuvettes (1 cm). Emission spectra were acquired on a HORIBA Jobin Yvon IBH FluoroLog-3 spectrofluorimeter, equipped with 3 slit double grating excitation & emission monochromators (2.1 nm/mm dispersion, 1200 grooves/mm). Spectra were reference corrected for both the excitation light source variation (lamp and grating) and the emission spectral response (detector and grating). Luminescence lifetimes were determined on a HORIBA Jobin Yvon IBH FluoroLog-3 spectrofluorimeter, adapted for multichannel scaling (MCS) measurements. A sub-microsecond Xenon flashlamp (Jobin Yvon, 5000XeF) was used as the light source, with an input pulse energy (100 nF discharge capacitance) of *ca*. 50 mJ, yielding an optical pulse duration of less than 300 ns at FWHM. Spectral selection was achieved by passage through a double grating excitation monochromator (2.1 nm/mm dispersion, 1200 grooves/mm). Emission was monitored perpendicular to the excitation pulse, again with spectral selection achieved by passage through a double grating excitation monochromator (2.1 nm/mm dispersion, 1200 grooves/mm). A thermoelectrically cooled single photon detection module (HORIBA Jobin Yvon IBH, TBX-04-D) incorporating fast rise time PMT, wide bandwidth preamplifier and picosecond constant fraction discriminator was used as the detector. Signals were acquired using an IBH DataStation Hub photon counting module and data analysis was performed using the commercially available DAS 6 decay analysis software package from HORIBA Jobin Yvon IBH.

Quantum yields were determined by the optically dilute method using the following equation;

$$\Phi_x/\Phi_r=[A_r(\lambda_r)/A_x(\lambda_x)]*[I_r(\lambda_r)/I_x(\lambda_x)]*[n_x^2/n_r^2]*[D_x/D_r]$$

where *A* is the absorbance at the excitation wavelength λ, *I* is the intensity of the excitation light at the same wavelength, *n* is the refractive index and *D* is the integrated luminescence intensity. The subscripts '*x*' and '*r*' refer to the sample and reference respectively. Quinine sulfate in 0.5 M sulfuric acid was used as the reference ($\Phi_r = 0.546$).

Circularly polarized luminescence and total luminescence spectra were recorded on an instrument described previously,[12–13] operating in a differential photon-counting mode. The light source for indirect excitation was a continuous wave 450 W xenon arc lamp from a Spex FluoroLog-2 spectrofluorometer, equipped with excitation and emission monochromators with dispersions of 4 nm/mm (SPEX, 1681B). Selective excitation of Tb(III) was accomplished with either a Coherent Innova-70 or Coherent Sabre TSM 15. The optical detection system consisted of a focusing lens, long pass filter, and 0.22 m monochromator. The emitted light was detected by a cooled EMI-9558B photomultiplier tube operating in photon-counting mode. All measurements were performed with quartz cuvettes with a path length of 0.4 or 1.0 cm.

Supplementary Material

Refer to Web version on PubMed Central for supplementary material.

Acknowledgments

The authors thank Michael D. Pluth for assistance with NMR spectra. M.S. thanks the German Research Foundation (DFG) for a research fellowship. G.M. thanks the National Institute of Health Minority Biomedical Research Support (2 S06 GM008192-27), Research Corporation Cottrell Science Award (CC6624), and the Henry Dreyfus Teacher-Scholar Award for financial support. A.J.I. thanks the Howard Hughes Medical Institute Award (52006312) for a research fellowship. This work was supported in part by NIH grant R01-HL69832 and by the Director, Office of Science, Office of Basic Energy Sciences, and the Division of Chemical Sciences, Geosciences, and Biosciences of the U.S. Department of Energy at LBNL under Contract No. DE-AC02-05CH11231.

References

1. Lakowicz, JR. Principles of Fluorescence Spectroscopy. Springer; Berlin: 2006. Wolfbeis, OS., editor. Fluorescence Spectroscopy: New Methods and Applications. Springer; Berlin: 1993.
2. Selected reviews: a)Parker D. Chem Soc Rev 2004;33:156–165.165 [PubMed: 15026820]b)Bünzli JCG, Piguet C. Chem Soc Rev 2005;34:1048–1077.1077 [PubMed: 16284671]c)Bünzli JCG. Acc Chem Res 2006;39:53–61.61 [PubMed: 16411740]d)de Bettencourt-Dias A. Curr Org Chem 2007;11:1460–1480.1480e)Gunnlaugsson T, Stomeo F. Org Biomol Chem 2007;5:1999–2009.2009 [PubMed: 17581643]f)Bünzli JCG. Chem Lett 2009;38:104–109.109g)Montgomery CP, Murray BS, New EJ, Pal R, Parker D. Acc Chem Res ASAP. 10.1021/ar800174z
3. For example: Perkin-Elmer: Delfia and LANCE, Cisbio: HTRF and Lumi4, Brahms: TRACE.
4. Reviews: a)Richardson FS, Riehl JP. Chem Rev 1977;77:773–792.792b)Riehl JP, Richardson FS. Chem Rev 1986;86:1–16.16c)Riehl JP, Richardson FS. Methods Enzymol 1993;226:539–553.553 [PubMed: 8277881]d)Brittain HG. Appl Spectr Rev 2000;35:175–201.201e)Dekkers HPJM. Berova N, Nakanishi K, Woody RW. Circular Dichroism. Wiley-VCHWeinheim2000f)Riehl JP, Muller G. Gschneidner KA, Bünzli J-CG, Pecharsky VK. Handbook on the Physics and Chemistry of Rare Earths 34North-Holland PublishingAmsterdam2005;
5. Dickins RS, Howard JAK, Maupin CL, Moloney JM, Parker D, Riehl JP, Siligardi G, Williams JAG. Chem Eur J 1999;5:1095–1105.
6. Di Bari L, Pintacuda G, Salvadori P, Dickins RS, Parker D. J Am Chem Soc 2000;122:9257–9264.
7. Bruce JI, Parker D, Lopinski S, Peacock RD. Chirality 2002;14:562–567. [PubMed: 12112329]

8. Poole RA, Bobba G, Cann MJ, Frias JC, Parker D, Peacock RD. Org Biomol Chem 2005;3:1013–1024. [PubMed: 15750644]
9. Leonard JP, Jensen P, McCabe T, O'Brien JE, Peacock RD, Kruger PE, Gunnlaugsson T. J Am Chem Soc 2007;129:10986–10987. [PubMed: 17696537]
10. Petoud S, Muller G, Moore EG, Xu J, Sokolnicki J, Riehl JP, Le UN, Cohen SM, Raymond KN. J Am Chem Soc 2007;129:77–83. [PubMed: 17199285]
11. Seitz M, Moore EG, Ingram AJ, Muller G, Raymond KN. J Am Chem Soc 2007;129:15468–15470. [PubMed: 18031042]
12. Bonsall SD, Houcheime M, Straus DA, Muller G. Chem Commun 2007;35:3676–3678.
13. Do K, Muller FC, Muller G. J Phys Chem A 2008;112:6789–6793. [PubMed: 18597442]
14. Montgomery CP, New EJ, Parker D, Peacock RD. Chem Commun 2008:4261–4263.
15. Lunkley JL, Shirotani D, Yamanari K, Kaizaki S, Muller G. J Am Chem Soc 2008;130:13814–13815. [PubMed: 18816117]
16. Gregolinski J, Starynowicz P, Hua KT, Lunkley JL, Muller G, Lisowski J. J Am Chem Soc 2008;130:17761–17773. [PubMed: 19053412]
17. New EJ, Parker D, Peacock RD. Dalton Trans 2009:672–679. [PubMed: 19378560]
18. Field JE, Muller G, Riehl JP, Venkataraman D. J Am Chem Soc 2003;125:11808–11809. [PubMed: 14505389]
19. a) Muller G, Riehl JP, Schenk KJ, Hopfgartner G, Piguet C, Bünzli JCG. Eur J Inorg Chem 2002:3101–3110. b) Muller G, Schmidt B, Jiricek J, Hopfgartner G, Riehl JP, Bünzli JCG, Piguet C. J Chem Soc, Dalton Trans 2001:2655–2662.
20. "H_4X" denotes the neutral ligand which is fully protonated at the four, relatively acidic hydroxyl groups (N-OH in 1,2-HOPO and phenolic OH in IAM). Consequently, "[Ln(HX)]" stands for a lanthanide complex with a triply deprotoned ligand.
21. Seitz M, Oliver AG, Raymond KN. unpublished results
22. Koscova S, Budesinsky M, Hodacova J. Collect Czech Chem Commun 2003;68:744–750.
23. Pei Y, Brade K, Brule E, Hagberg L, Lake F, Moberg C. Eur J Org Chem 2005:2835–2840.
24. Xu J, Durbin PW, Kullgren B, Ebbe SN, Uhlir LC, Raymond KN. J Med Chem 2002;45:3963–3971. [PubMed: 12190318]
25. a) Petoud S, Cohen SM, Bünzli JCG, Raymond KN. J Am Chem Soc 2003;125:13324–13325. [PubMed: 14583005] b) Samuel APS, Moore EG, Melchior M, Xu J, Raymond KN. Inorg Chem 2008;47:7535–7544. [PubMed: 18671388]
26. a) Moore EG, Xu J, Jocher CJ, Werner EJ, Raymond KN. J Am Chem Soc 2006;128:10648–10649. [PubMed: 16910637] b) Moore EG, Xu J, Jocher CJ, Castro-Rodriguez I, Raymond KN. Inorg Chem 2008;47:3105–3118. [PubMed: 18311915] c) D'Aleo A, Xu J, Moore EG, Jocher CJ, Raymond KN. Inorg Chem 2008;47:6109–6111. [PubMed: 18553909]
27. The assignment of water molecules to the inner coordination sphere is based on the luminescence lifetime measurements in H_2O and D_2O (see Table 1).
28. a) Knof U, von Zelewsky A. Angew Chem Int Ed 1999;38:303–322. b) Aspinall H. Chem Rev 2002;102:1807–1850. [PubMed: 12059255] c) Di Bari L, Salvadori P. Coord Chem Rev 2005;249:2854–2879.
29. Beeby A, Clarkson IM, Dickins RS, Faulkner S, Parker D, Royle L, de Sousa AS, Williams JAG, Woods M. J Chem Soc, Perkin Trans 2 1999;3:493–504.
30. Horrocks WD Jr, Sudnick DR. Acc Chem Res 1981;14:384–392.
31. Luk CK, Richardson FS. J Am Chem Soc 1975;97:6666–6675.

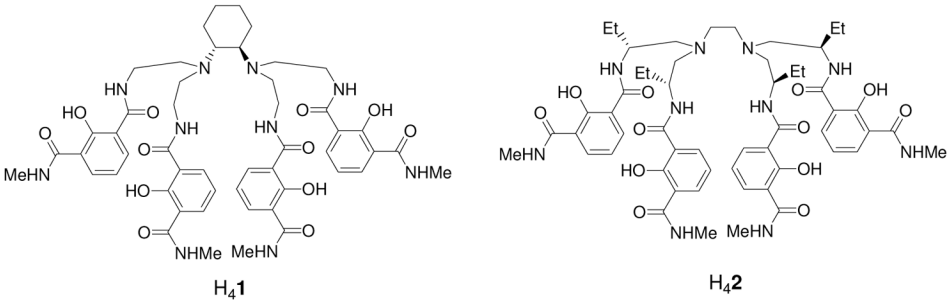

Figure 1.
Ligands based on 2-hydroxyisophthalamides (IAM).

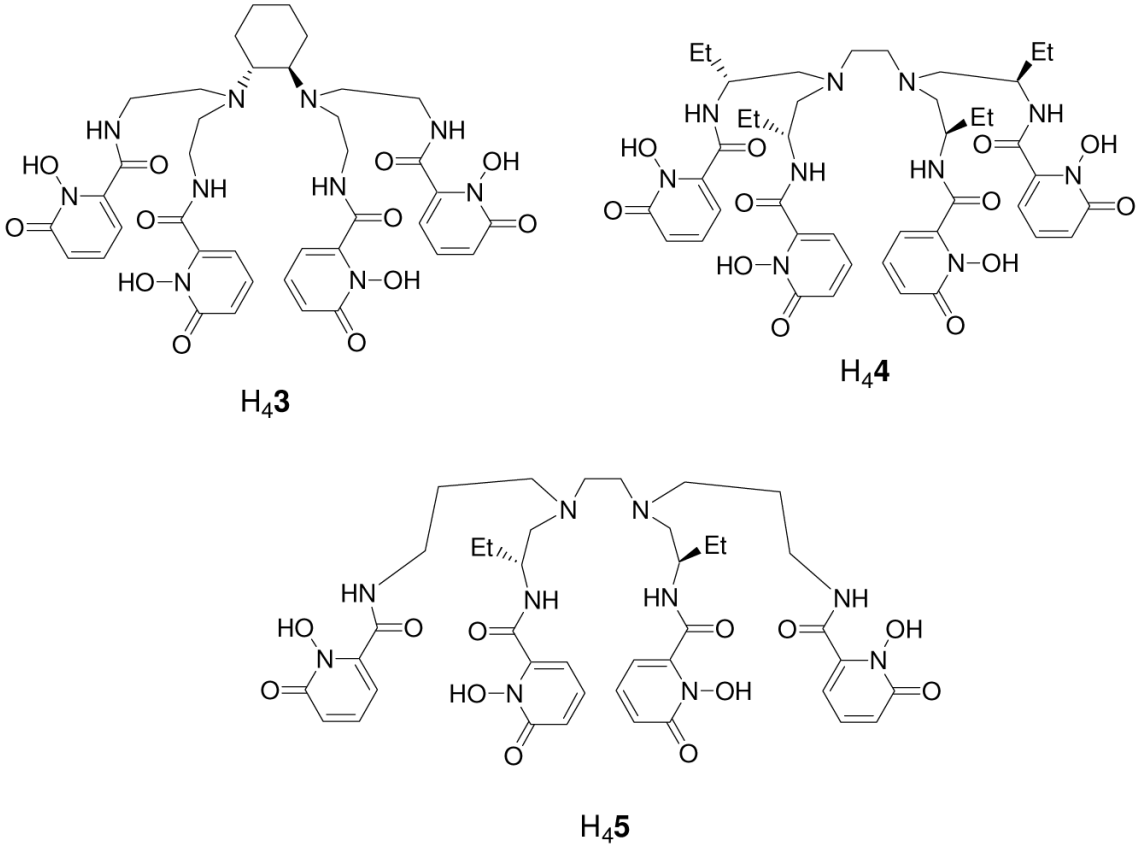

Figure 2.
Ligands based on 1-hydroxy-2-pyridinone (1,2-HOPO).

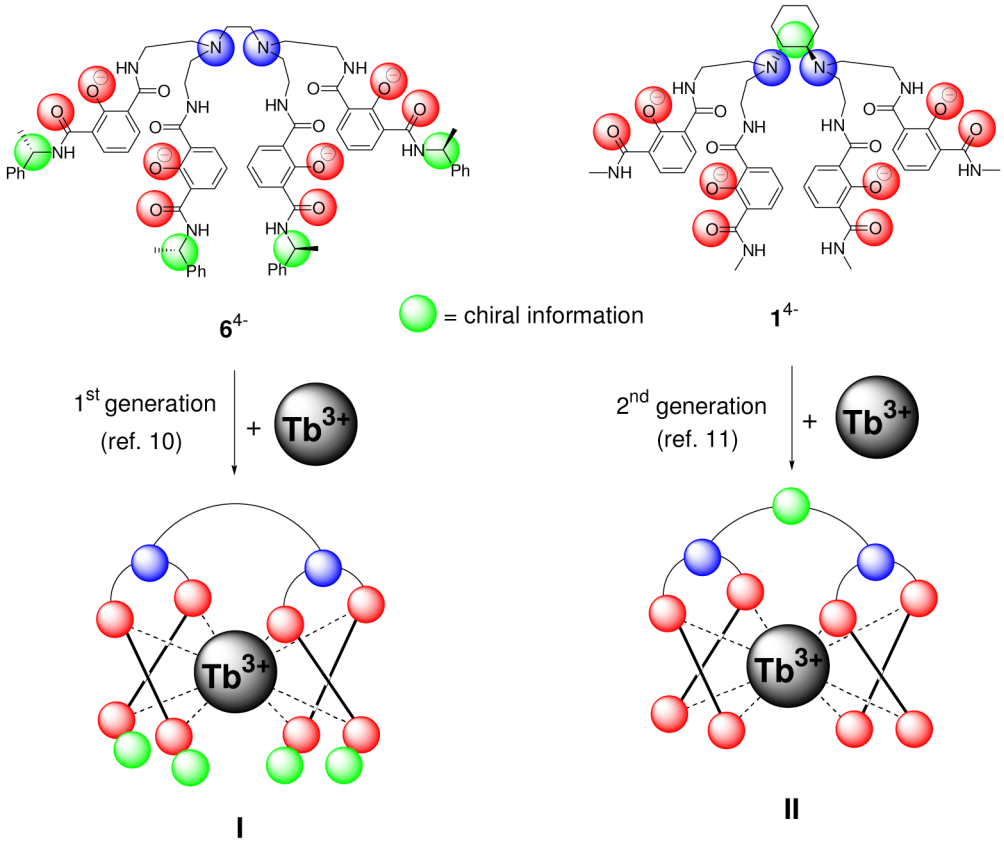

Figure 3.

Schematic representation of the design change for the 1st to the 2nd generation of enantiopure, octadentate ligands: Chiral information (green spheres) in the polyamine backbone for **II** (blue part) instead of incorporation into the chelating IAM moiety in **I** (red part).

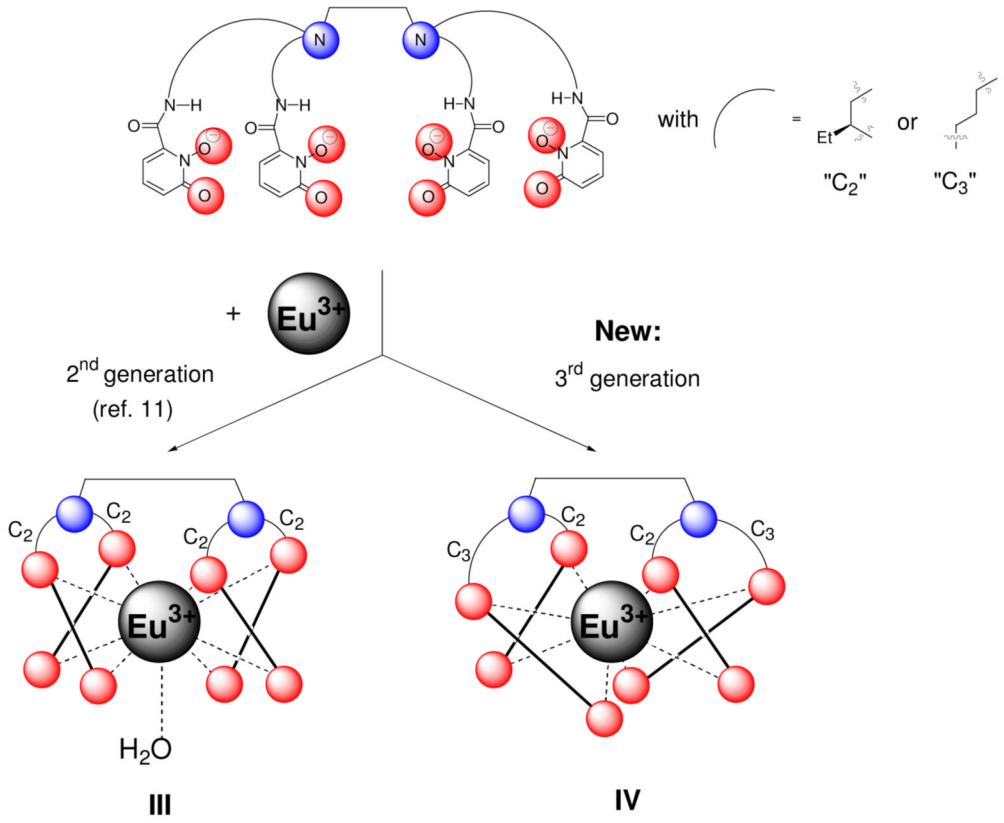

Figure 4.

Schematic representation of the design principle for the 3rd generation of chiral, octadentate 1,2-HOPO ligands for europium luminescence: Blocking of the bottom coordination site for water molecules through longer ligand arms (C_3 unit vs. C_2 unit).

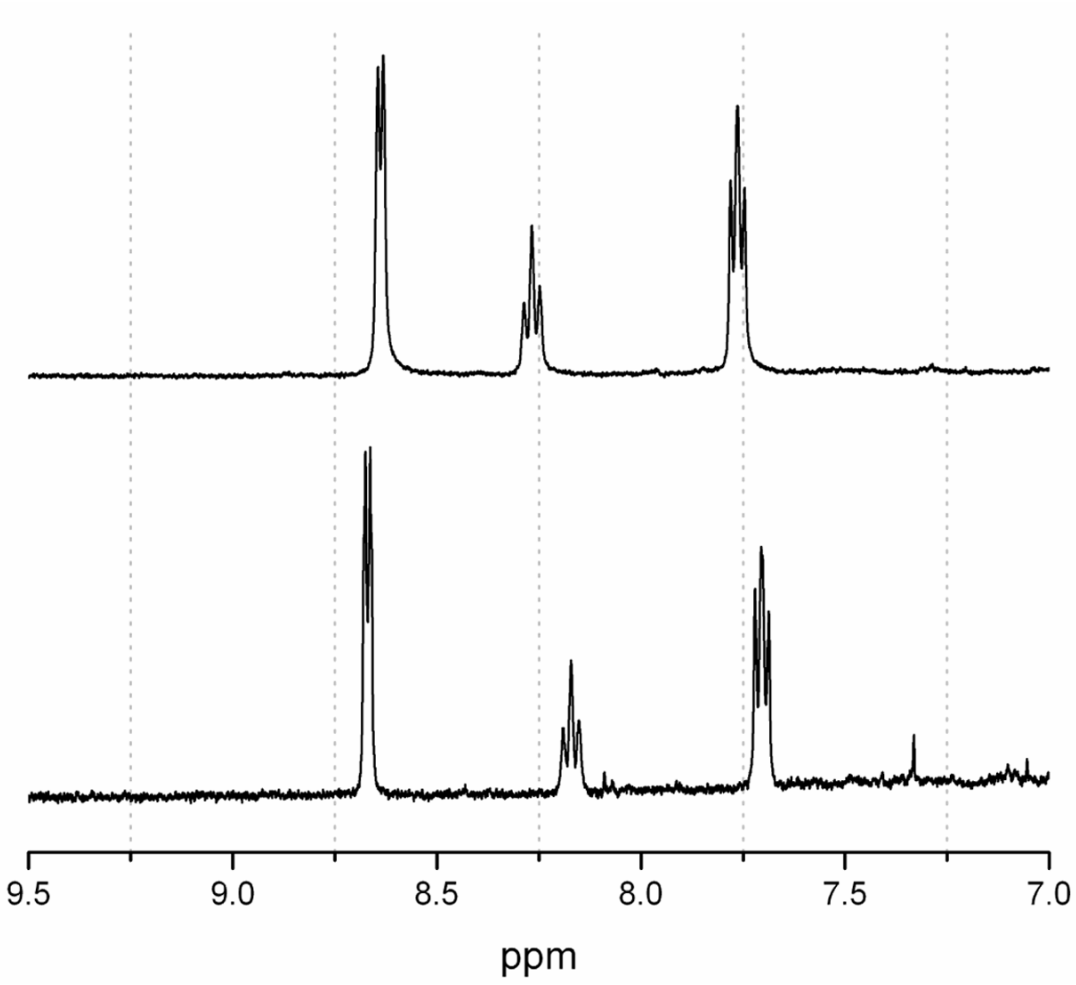

Figure 5.
Aromatic region of the ^{1}H NMR spectra (500 MHz) of saturated solutions of [Eu(H**3**)(H_2O)] (top) and [Eu(H**4**)(H_2O)] (bottom)[11] in CD_3OD.

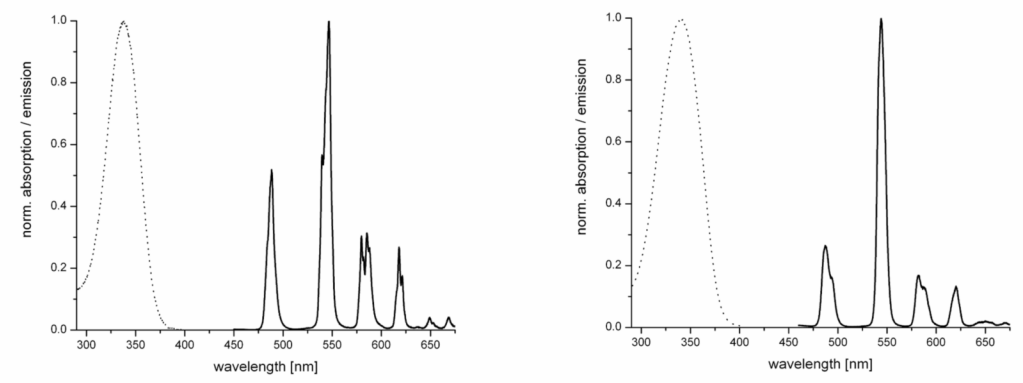

Figure 6.

Normalized absorption (dotted lines) and steady-state emission (solid lines) of [Tb(H**1**)] (left, λ_{exc} = 340 nm) and [Tb(H**2**)(H_2O)] (right, λ_{exc} = 340 nm) in 0.1 M aqueous Tris buffer at pH 7.4.

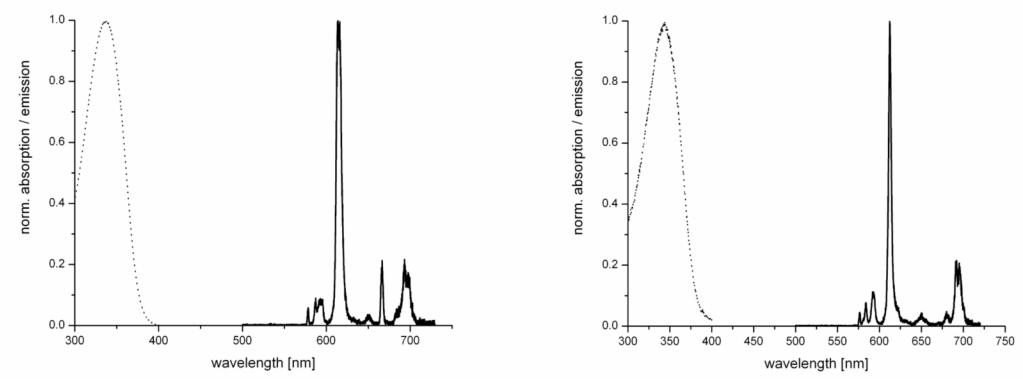

Figure 7.
Normalized absorption (dotted lines) and steady-state emission (solid lines) of [Eu(H**3**)(H_2O)] (left, λ_{exc} = 328 nm) and [Eu(H**4**)(H_2O)] (right, λ_{exc} = 340 nm) in 0.1 M aqueous Tris buffer at pH 7.4.

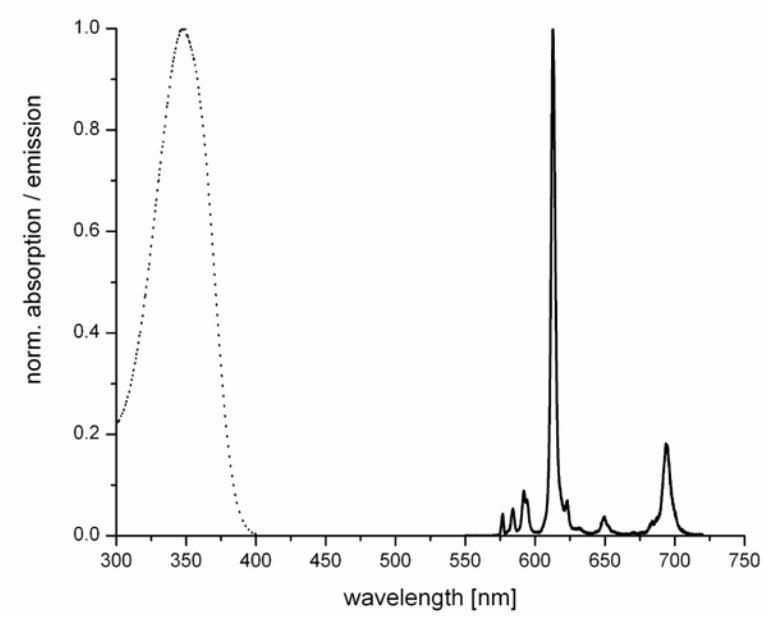

Figure 8.
Normalized absorption (dotted line) and steady-state emission (solid line, λ_{exc} = 347 nm) of [Eu(H**5**)(H_2O)] in 0.1 M Tris buffer (pH 7.4)/MeOH (1:9, v/v).

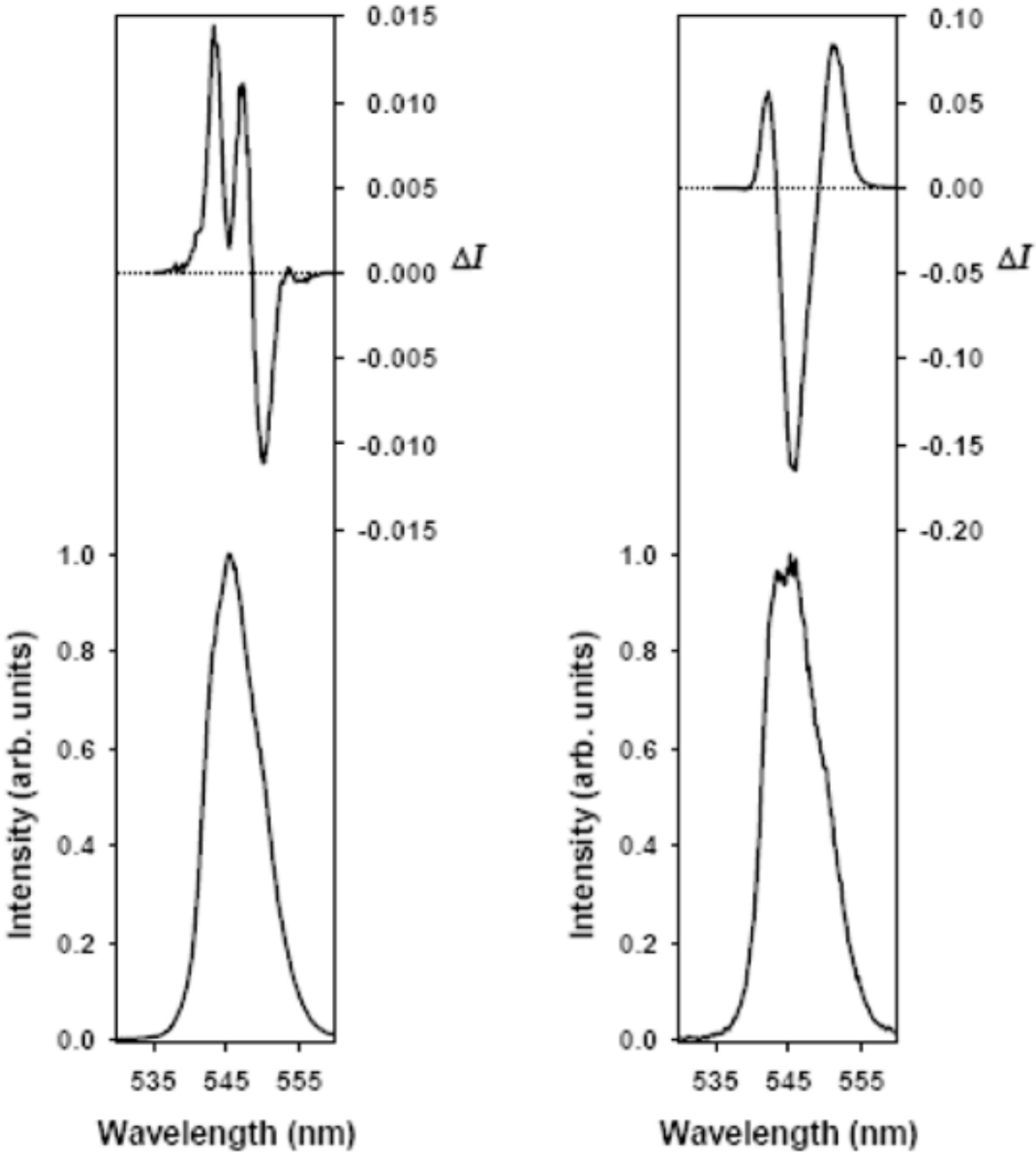

Figure 9.

CPL (top) and total luminescence (bottom) spectra of the $^5D_4 \rightarrow {}^7F_5$ transition of [Tb(H**2**)(H_2O)] in MeOH (left: c ≈ 1 mM, excitation at λ = 360 nm) and in 0.1 M Tris buffer at pH 7.4 (right: saturated solution, excitation at λ = 346 nm).

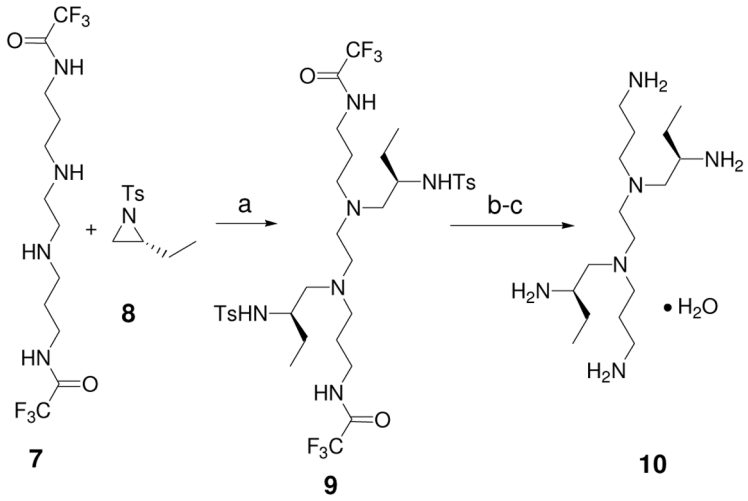

Scheme 1.

Synthesis of the enantiopure, tetrapodal hexamine backbone **10**.

a) Benzene, 56%; b) HBr (48%)/HOAc; c) Dowex 1x8 (HO^-), H_2O, 54% (from 9).

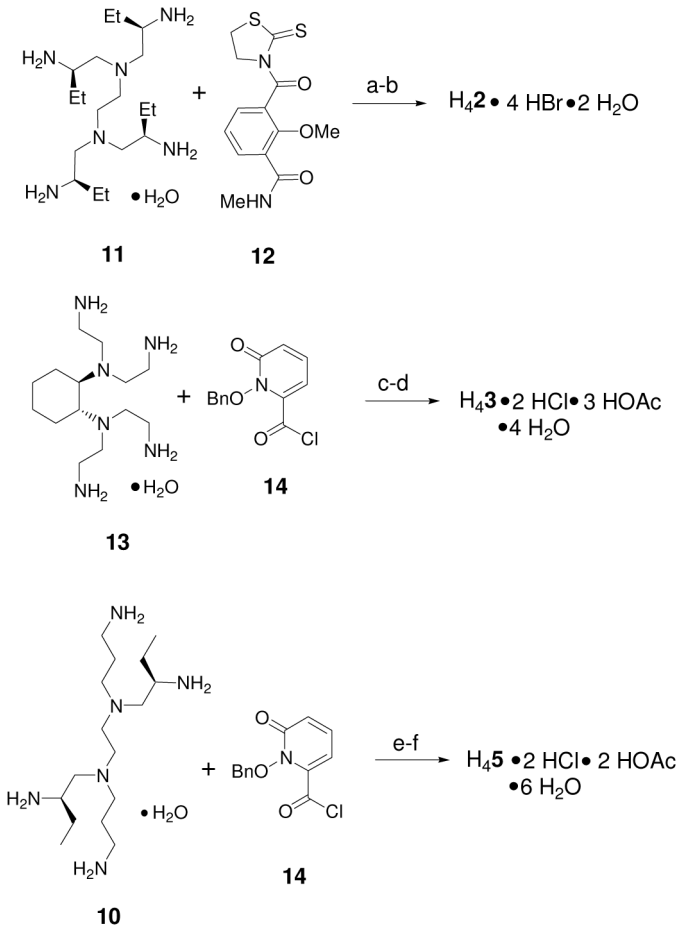

Scheme 2.

Assembly of the new octadentate ligands H_4**2**, H_4**3**, and H_4**5**.

a) NEt_3, CH_2Cl_2, 39%; b) BBr_3, CH_2Cl_2, 63%; c) NEt_3, CH_2Cl_2, 58%; d) HCl/HOAc, 74%; e) NEt_3, CH_2Cl_2, 34%; f) HCl/HOAc, 97%.

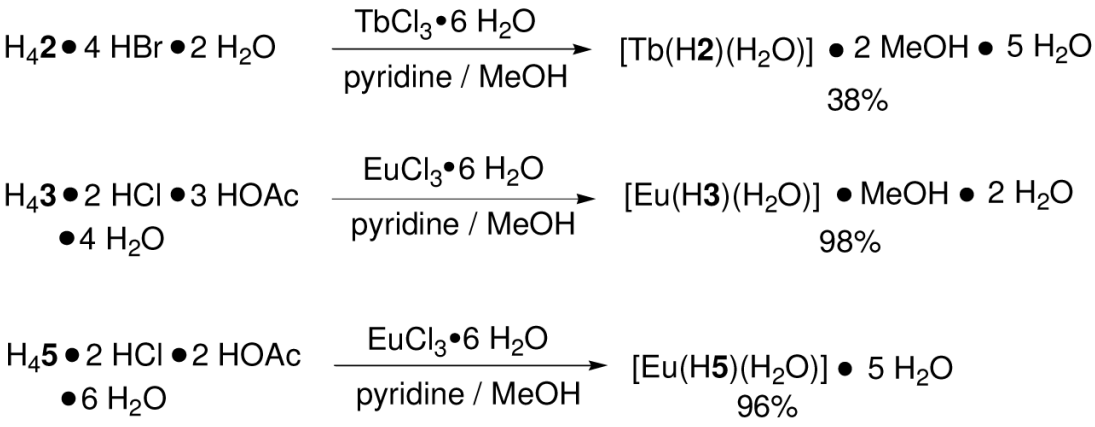

Scheme 3.
Complex synthesis.

Table 1

General photophysical parameters of the lanthanide complexes in solution (0.1 M Tris buffer, pH 7.4).

Complex[a]	λ_{max} [nm]	λ_{exc} [nm]	Φ[d]	τ (H_2O) [ms]	χ^2	τ (D_2O) [ms]	χ^2	q[e]
[Tb(H**1**)][b]	337	340	0.57	2.28	1.07	2.59	1.02	−0.04
[Tb(H**2**)(H_2O)]	340	340	0.30	0.63 (26%) 1.54 (74%)	1.07	1.01 (12%) 2.49 (88%)	1.06	2.6 1.0
[Eu(H**3**)(H_2O)]	337	328	0.048	0.19 (27%) 0.50 (73%)	1.10	0.35 (16%) 1.28 (84%)	1.02	2.6 1.2
[Eu(H**4**)(H_2O)][b]	344	340	0.077	0.48	1.13	0.88	1.11	0.84
[Eu(H**5**)(H_2O)][c]	347	347	0.081	0.57 (0.69)[f]	1.09 (1.08)[f]	(0.85)[f]	(1.05)[f]	(0.57)[f]

[a] Assignment of water molecules based on the q determinations (last column) for the major species in solution.

[b] Ref. 11;

[c] In 0.1 M Tris (pH 7.4)/MeOH (1:9, v/v);

[d] ±15%, using quinine sulfate (Φ = 0.546) in 0.5 M sulfuric acid as standard;

[e] q = number of solvent molecules bound to the lanthanide; Ref. 29;

[f] In CH_3OH or CD_3OD.

Table 2

Circularly polarized luminescence of the lanthanide complexes at 295 K.

Complex	Electronic transition	λ_{exc} [nm]	λ [nm] (0.1M Tris, pH 7.4)	g_{lum}	λ_{exc} [nm]	λ [nm] (MeOH)	g_{lum}
[Tb(H**1**)][a]	$^5D_4 \rightarrow {}^7F_5$	350	543.6 545.8 551.0	−0.083 +0.078 −0.051	352	543.8 545.8 551.0	−0.043 +0.052 −0.033
[Tb(H**2**)(H_2O)]	$^5D_4 \rightarrow {}^7F_5$	346	542.0 545.6 551.2	+0.14 −0.34 +0.40	360	543.2 547.0 550.0	+0.036 +0.026 −0.041
[Eu(H**3**)(H_2O)]	$^5D_0 \rightarrow {}^7F_1$	n.a.	n.a.	n.a.	354	589.4 593.6 596.6	−0.073 +0.053 −0.17
[Eu(H**4**)(H_2O)]a	$^5D_0 \rightarrow {}^7F_1$	360	586.6 594.2	−0.046 −0.12	360	591.0 596.6	−0.097 −0.20
[Eu(H**5**)(H_2O)]	$^5D_0 \rightarrow {}^7F_1$	n.a.	n.a.	n.a.	357	589.6 593.6 596.2	−0.064 +0.081 −0.12

[a]Ref. 11.